Proceeding of the Korean Nuclear Society Autumn Meeting
Seoul Korea October 1998

Simple Analytical Model for Predicting Onset of Helical OTSG Instability

Han-Ok Kang, Hwan-Yeol Kim, Ju-Hyeon Yoon,
Joo-Pyung Kim, Doo Jeong Lee
Korea Atomic Energy Research Institute
P.O. Box 105, Yuseong, Taejeon, Korea, 305-600

Abstract

A simple model to analyze helical once-through steam generators (OTSG) instability has been developed. The model is formulated with control volumes having moving boundaries. The constant pressure drop boundary condition is applied to both ends of coiled tube and the homogeneous equilibrium flow model is used for the two-phase region. Shell-side energy conservation is also considered and heat fluxes in the each region are treated as variables.

The governing equations were nondimensionalized and perturbed after some manipulation. The helical OTSG stability criterion was then developed through application of general stability criterion to the first order perturbed equations. The steady-state results were obtained using the developed model. The results and Nariai's experimental data were found in good agreement. The calculated threshold inlet throttling coefficients with heat flux variation show similar trends with the experimental data. The result shows that a large amount of inlet throttling coefficients is needed if feedwater flow rate is low.

1. Introduction

Once-through steam generators have advantages that are compact and produce superheated steam without steam separator. Particularly, adoption of helical coils offers more compactness, structural stability and makes tubes to compensate for the thermal expansion of themselves[1]. Integral reactors and liquid metal fast breeder reactors(LMFBR) have been favorite application fields of the helical once-through steam generators(OTSG). SMART(System-integrated Modular Advanced ReacTor) which are being now developed by KAERI also includes helical OTSGs to produce steam. It was known that the unstable flow conditions of tube-side flow might cause flow oscillations of constant or diverging amplitude[2]. These oscillations could disturb control systems or cause mechanical damage. The study on design and operating conditions preventing flow instability should precede the application of helical OTSG to reactors.

There have been a few of experimental studies on helical OTSG instabilities with related to development of LMFBR and integral reactors. Waszink, Kubota and Unal conducted experiments for the LMFBR steam generators[3,4,5]. Kozeki and Nariai did for the steam generators of integral reactor[6,7,8]. From the experimental data, some derived correlations to predict threshold conditions. However, until now, important non-dimensional numbers governing helical OTSG instabilities or instability maps were not well defined yet and the usefulness of the correlations are very restricted.

Clausse and Lahey developed homogeneous equilibrium model using nodal method with moving boundaries for the modeling of a BWR loop[9]. Later, Chang and Lahey extended former study by including diabatic two-phase flow model and point neutron kinetics model[10]. In the work presented here, the nodal method is applied to helical OTSG instability that includes the superheated region dynamics. Shell-side energy conservation equations are included and heat fluxes are treated as variables. First linearized model is developed and used to predict the threshold inlet throttling coefficients, which is compared with experimental data. Second, several hydraulic characteristics of limit cycle beyond the threshold conditions are studied with non-linear model.

2. Analysis

2.1 Governing equations

It was known from the former studies that the effect of others on a tube could be approximately substituted to constant pressure drop condition, when dozens of tubes had common headers at both ends[11]. This assumption is adopted in this study and the others are as follow:

(a) Heat flux of steam generators is generally much lower than those of BWR cores, which makes the nucleate boiling point in the tube to approach to the bulk saturation point. The sub-cooled nucleate boiling is not considered and thermal equilibrium between two phases is assumed.

(b) Film dry-out was known to occur before fluid quality became to be one for the high flow rate. Dry-out quality is assumed one in this study for the simplicity.

(c) If primary fluid is well mixed and has a high heat capacity, the effect of interaction is not large and primary temperature can be assumed to be time invariant. Oscillation of primary side is not considered.

(d) Tube wall heat capacity is neglected. It was evident through simple time-scale analysis that the time scale related to tube wall dynamics is very short relative to residence time in the tube.

(e) Negligible viscous dissipation, kinetic energy, potential energy an flow work in the energy equation

(f) Only instability in the one module is objective of this study and the system instability is not considered. So constant inlet temperature is given.

Fig. 1 shows computational domain and the definitions of parameters used in this study. The domain includes both primary and secondary sides. Secondary side is composed of sub-cooled, two-phase and superheated regions. Heat fluxes in each region are calculated from log-mean temperature differences. Overall secondary pressure drop is maintained to be constant. The length scale of secondary side is tube total length L_{SG} and that of primary side is H_{SG}.

The primary fluid temperature distribution is needed for the heat flux calculation. Simplified steady energy conservation equations are utilized for the purpose. Based on above assumptions, the secondary side mass and energy conservation equations of the HEM defined in each region can be expressed as follows.

Sub-cooled region

$$\rho_f \frac{dl_f}{dt} = \rho_i j_i - \rho_b j_b \tag{1}$$

$$\rho_f \frac{dl_f h_f}{dt} = \rho_i h_i j_i - \rho_b h_b j_b + \frac{q'_f l_f}{A_s} \tag{2}$$

Two-phase region

$$\rho_t \frac{dl_t}{dt} = \rho_b j_b - \rho_d j_d \tag{3}$$

$$\rho_t \frac{dl_t h_t}{dt} = \rho_b h_b j_b - \rho_d h_d j_d + \frac{q'_t l_t}{A_s} \tag{4}$$

Superheated region

$$\rho_v \frac{dl_v}{dt} = \rho_d j_d - \rho_e j_e \tag{5}$$

$$\rho_v \frac{dl_v h_v}{dt} = \rho_d h_d j_d - \rho_e h_e j_e + \frac{q'_v l_v}{A_s} \tag{6}$$

Following constitutive relations are applied to the above equations.

$$n_f = \frac{n_i + n_b}{2}, \quad n_t = \frac{n_b + n_d}{2}, \quad n_v = \frac{n_d + n_e}{2} \tag{7}$$

$$h_f = \frac{h_i + h_b}{2}, \quad h_t = \frac{h_b + h_d}{2}, \quad h_v = \frac{h_d + h_e}{2} \tag{8}$$

$$L_{SG} = l_f + l_t + l_v \tag{9}$$

The node specific volumes and enthalpies of each control volumes are approximated to be the averages of inlet and exit values of the control volumes, which assumption leads to Eq. (8) and Eq. (9). Momentum conservation equation is setup over the whole tube length.

$$\begin{aligned}\Delta p_{ext} = {} & \frac{1}{2}\frac{d}{dt}\left(r_i j_i + r_b j_b'\right)\cdot l_f + \frac{1}{2}\frac{d}{dt}\left(r_b j_b' + r_d j_d'\right)\cdot l_t + \frac{1}{2}\frac{d}{dt}\left(r_d j_d' + r_e j_e\right)\cdot l_v + r_e j_e^2 - r_i j_i^2 \\ & + g\left(r_f l_f' + r_t l_t' + r_v l_v'\right) + \frac{1}{2}k_i r_i j_i^2 + \frac{1}{4D_i}\left\{f_f l_f\left[r_i j_i^2 + r_b j_b'^2\right] + 2 f_t l_t r_b\left[r_i j_b'^2 + (1-r_i)R_j j_d'^2\right]\right. \\ & \left. + f_v l_v\left[r_d j_d'^2 + r_e j_e^2\right]\right\}\end{aligned} \tag{10}$$

Above equation can be derived by integrating genearl equation with linear profile assumption. The equation includes the inlet throttling term which plays critical rule to stabiliize the helical OTSG. In case of two-phase kinetic energies, weighting factor r_i is introduced for the generality. The value is mainly dependent on heat flux profile in the two-phase region. The heat flux are reported to be almost constant in the two-phase region of helical OTSG and r_i is assumed to be one in this study[6]. Velocities relative to moving boundaries are used in the mass and energy equations. On the other hand, momentum equation is expressed as real velocities. Heat flux are calculated from LMTD(log mean temperature difference) in the each region[12]. The heat transfer coefficients are defined in the outer surface of tube and compsed of three components.

The single-phase friction factor for the coiled tube is determined from Colebrook's correlation for the straight tube and Ito's correction factor for the coiled tube[8]. Two-phase friction pressure drop ΔP_t is given by the single-phase friction pressure drop ΔP_{f0} assuming all the flow in water phase, multiplied by a coefficient Kozeki's two-phase multiplier Φ_{f0}[6]. Heat transfer coefficients for the tube side are determined from Mori-Nakayama's and Kozeki's correlations for the single-phase and two-phase regions respectively[6,13].

2.2 Nondimensionalization

To treat the problems of helical OTSG instability, we can non-dimensionalized the conservation equations to identify relevant dimensionless parameters. The nondimensional numbers and reference quantities used in this study are following.

$$R_{ib} = \frac{r_i}{r_b}, R_{if} = \frac{r_i}{r_f}, R_{it} = \frac{r_i}{r_t}, R_{id} = \frac{r_i}{r_d}, R_{iv} = \frac{r_i}{r_v}, R_{ie} = \frac{r_i}{r_e}, R_{ev} = \frac{r_e}{r_v},$$

$$R_i = \frac{n_i}{n_{db}}, R_f = \frac{n_f}{n_{db}}, R_t = \frac{n_t}{n_{db}}, R_d = \frac{n_d}{n_{db}}, R_v = \frac{n_v}{n_{db}}, R_e = \frac{n_e}{n_{db}}, R_{ii} = \frac{n_b - n_i}{n_i}, R_j = \left(\frac{r_d}{r_b}\right)^2,$$

$$R_D = \frac{L_{SG}}{2D_i}, R_H = \frac{H_{SG}}{L_{SG}}, N_{sub} = \frac{h_{bi}}{h_{db}}\frac{n_{db}}{n_f}, N_{pch} = \frac{q_r' L_{SG}}{A_s j_r}\frac{n_{db}}{h_{db}}, Eu = \frac{\Delta P_{ext}}{1/2\, r_i j_i^2}, k_i = \frac{\Delta P_{orifice}}{1/2\, r_i j_i^2},$$

$$Fr = \frac{j_r^2}{g L_{SG}}, L_r = \frac{L_{SG}}{N_{pch}}, t_r = \frac{L_r}{j_r}, q_r' = \frac{A_p m_p c_{pi} \Delta T_r}{L_{SG}}, T_r = T_{pi} - T_{si},$$

$$\hat{j}_i = \frac{j_i}{j_r}, \hat{l}_f = \frac{l_f}{L_r}, \hat{l}_t = \frac{l_t}{L_r}, \hat{l}_v = \frac{l_v}{L_r}, \hat{q}_f' = \frac{q_f'}{q_r'}, \hat{q}_t' = \frac{q_t'}{q_r'}, \hat{q}_v' = \frac{q_v'}{q_r'}, \hat{t} = \frac{t}{t_r} \tag{11}$$

Above nondimensional parameters are including density ratios, length ratio, N_{sub}, N_{pch}, Eu, Fr and k_i. Density ratios have large variations with system pressure. The subcooling number, N_{sub} takes into account the time-lag effect in the liquid region due to the subcooling of the fluid. The phase-change number, N_{pch} scales the change of phase due to the heat transfer to the secondary medium in the two-phase region. The N_{sub} and N_{pch} are known to be important parameters of BWR core instability[14]. The R_H and Fr are related to the gravity effect which is not large except for the very low mass flow rate. The resulting nondimensional state equations are following.

$$d_0\frac{d\hat{j}_i}{d\hat{t}} = d_1\frac{d\hat{l}_f}{d\hat{t}} + d_2\frac{d\hat{l}_t}{d\hat{t}} + \frac{R_D}{N_{pch}}\left\{ f_f\hat{l}_f\left[\hat{j}_i^2 + \frac{\hat{j}_b'^2}{R_{ib}}\right] + 2f_t\hat{l}_t\frac{1}{R_{ib}}\left[r_i\hat{j}_b'^2 + (1-r_i)R_j\hat{j}_d'^2\right] + f_v\hat{l}_v\left[\frac{\hat{j}_d'^2}{R_{id}} + \frac{\hat{j}_e^2}{R_{ie}}\right]\right\}$$
$$+ \frac{2R_H}{N_{pch}Fr}\left(\frac{\hat{l}_f}{R_{if}} + \frac{\hat{l}_t}{R_{it}} + \frac{\hat{l}_v}{R_{iv}}\right) + 2\left(\frac{\hat{j}_e^2}{R_{ie}} - \hat{j}_i^2\right) + k_i r_i j_i^2 - Eu \tag{12}$$

$$\frac{d\hat{l}_f}{d\hat{t}} = 2R_{if}\hat{j}_i - 2\frac{R_{if}}{N_{sub}}\hat{q}_f'\hat{l}_f \tag{13}$$

$$\frac{d\hat{l}_t}{d\hat{t}} = -2R_{it}\hat{j}_i + 4\frac{R_{it}}{N_{sub}}\hat{q}_f'\hat{l}_f - 2R_t\hat{q}_t'\hat{l}_t \tag{14}$$

$$g_0\frac{d\hat{h}_{ed}}{d\hat{t}} = g_1\hat{j}_i\hat{h}_{ed} + g_2\hat{l}_f\hat{h}_{ed} + g_3\hat{l}_t\hat{h}_{ed} + g_4\hat{l}_f + g_5\hat{l}_t + g_6 + \Psi \tag{15}$$

New coefficients are introduced in the Eq. (15). These four state equations are used for the instability study. There is one point to be additionally mentioned which is that j_i, ι_f and l_t are coupled explicitly but h_{ed} has implicit effect on other valiables through exit properties.

2.3 Linear analysis

Standard linear analysis is applied the above equations (Rowland, 1986). The nondimensional variables are first seperated to steady and perturbed values and then substituted to the state equations. The obtained 0^{th} order equations are rearranged and can be expressed as follows.

$$Eu = f_1\hat{j}_i^2\hat{l}_f + f_2\hat{j}_i^2\hat{l}_t + f_3\hat{j}_i\hat{l}_f^2 + f_4\hat{j}_i\hat{l}_f\hat{l}_t + f_5\hat{j}_i\hat{l}_t^2 + f_6\hat{l}_f^3 + f_7\hat{l}_f^2\hat{l}_t + f_8\hat{l}_f\hat{l}_t^2 + f_9\hat{l}_t^3 + f_{10}\hat{j}_i^2$$
$$+ f_{11}\hat{j}_i\hat{l}_f + f_{12}\hat{j}_i\hat{l}_t + f_{13}\hat{l}_f^2 + f_{14}\hat{l}_f\hat{l}_t + f_{15}\hat{l}_t^2 + f_{16}\hat{j}_i + f_{17}\hat{l}_f + f_{18}\hat{l}_t + f_{19} \tag{16}$$

$$\hat{l}_f = \frac{N_{sub}}{\hat{q}_f'}\hat{j}_i \tag{17}$$

$$\hat{l}_t = \frac{1}{R_i\hat{q}_t'}\hat{j}_i \tag{18}$$

$$\hat{h}_{ed} = -\left(g_4\hat{l}_f + g_5\hat{l}_t + g_6\right)/\left(g_1\hat{j}_i + g_2\hat{l}_f + g_3\hat{l}_t\right) \tag{19}$$

Though Eu is generally known parameter and j_i obtained from it, the j_i is fixed to be one and Eu is calculated from the Eq. (16) in this study. For the given j_i, the ι_f, l_t and h_{ed} can be determined from the above equations. The coefficients in the above equations include heat flux terms which are dependent on primary condition. Primary fluid flows in the opposite diretion of secondary medium so that the temperaute of primary fluid at the tube inlet is unknown. Tube exit pressure are given as input and values at other points are obtained considering pressure drop. Properties are calculated from the pressure and temperature varying at each point. So the converged steady solution needs two kinds of iteration, one is inner iteration for pressure levels and other outer iteration for heat flux at each point. The obtained steady state values of each variables are used in the stability analysis. The 1^{th} order pertubation equations can be expressed as follows.

$$A_0 \frac{d\hat{j}_i}{d\hat{t}} = A_1 \hat{j}_i + A_2 \hat{l}_f + A_3 \hat{l}_t + A_4 \hat{h}_{ed} \tag{20}$$

$$\frac{d\hat{l}_f}{d\hat{t}} = B_1 \hat{j}_i + B_2 \hat{l}_f \tag{21}$$

$$\frac{d\hat{l}_t}{d\hat{t}} = C_1 \hat{j}_i + C_2 \hat{l}_f + C_3 \hat{l}_t \tag{22}$$

$$D_0 \frac{d\hat{h}_{ed}}{d\hat{t}} = D_1 \hat{j}_i + D_2 \hat{l}_f + D_3 \hat{l}_t + D_4 \hat{h}_{ed} \tag{23}$$

The state equations are Laplace-transformed and a characteristic equation is derived. Routh-Hurwitz criterion is applied to the characteristic equation to obtain the instability boundary condition[15].

3. Results and discussion

The steady results are compared with Nariai's experimental data. The experimental conditions are shown in the Table 1. The lengths of sub-cooled and two-phase regions are calculated with varying inlet sub-cooling temperature and feedwater mass flow rate. Fig. 2 shows the calculated results and experimental data together. The calculated results have almost same trends with experimental data in the figure. The length of two-phase region increases with increasing mass flow rate but does not nearly change in spite of large change of inlet sub-cooling degree. The pressure drop in the sub-cooled region is insignificant except that induced by inlet orifice and pressure drops in the two-phase and superheated region takes most part of total pressure drop. Fig.3 shows the trend of total pressure drop and each pressure drop components. The pressure drop in the sub-cooled region without orifice is too small to be distinguished from other components. Total pressure drop has a positive gradient in the figure, which shows the oscillations shown later is not Ledinegg type instability. As the mass flow rate increases, pressure drop in the superheated region itself increases, but the portion which it takes in the total pressure drop decreases.

We obtain the threshold inlet throttling coefficients adapting the stability criterion to linearized model. Two kinds of calculations are conducted. One is done with heat flux perturbation terms and other without the perturbation. By comparing two results, we can understand the role of heat flux perturbation in the helical OTSG instability. Nariai express the threshold inlet throttling coefficients only as a function of the fraction of two-phase region length in the total tube length, l_t/L_{SG}. Until now, there have been no general helical OTSG instability maps. Each researcher expressed their experimental data using parameters of themselves. For example, Ishii used N_{pch} and N_{sub}, while Unal used exit quality. The ratios of pressure drops in the sub-cooled region and two-phase region were used in the some Russian literatures.

Fig. 4 shows threshold inlet throttling coefficients as a function of l_t/L_{SG}. Symbols are from experiments and lines from calculations. Left down part of the figure is unstable region and right upper part is stable region. Thick lines are obtained with heat flux perturbation, while thin lines without the perturbation. The comparison of two results shows the strong stabilizing effect of flux perturbation. Particularly, heat flux variation in the sub-cooled region plays a important rule. The role of heat flux variation in the helical OTSG is thought to be very different from that in the BWR core instability. Thick lines have similar trends with symbols in the figure. Particularly, experimental points and calculated results show steep increase at the low l_t/L_{SG}. The length of two-phase region is proportional to feedwater mass flow rate in the Fig. 2. Above characteristics of helical OTSG instability shows that it is very difficult to prevent flow instability in the low feedwater flow rate.

4. Conclusion

Simple analytical models to study helical OTSG instability are developed in this study. Steady state characteristics are compared with Nariai's experimental data. The calculated results of the length of each region and pressure drops show almost same trends with experimental data. Total pressure drop expressed as a function of mass flow rate has a positive gradient, which shows the instability emerging in the calculation condition is not Ledinegg type instability. It is confirmed that heat flux variation has a strong stabilizing effect from the result from the linearized analysis. The calculations considering heat flux variation make the results to approach to the experimental data and show that a large amount of inlet throttling coefficients is needed in the low mass flow rate. The developed model can be used to determine SMART helical OTSG orifice size in the future.

Acknowledgement

This project has been carried out under the Nuclear R&D Program by MOST.

References

[1] H. O. Kang et al, Review of two-phase instabilities, Korea Atomic Energy Institute, KAERI/AR-469/97, June, 1997.
[2] I.I. Belyakov et al., Hydraulic stability of steam-forming elements in convective heating, transformed from Atomnaya Energiya 65(1) (1988) 12-17.
[3] R.P. Waszink and L.E. Efferding, Hydrodynamic stability and thermal performance tests of a 1-MWt Sodium-heated once-through steam generator model, ASME paper 73-pwr-16 (1973).
[4] Kubota and T. Tsuchiya, Hydrodynamic stability tests and analytical model development for once-through Sodium heated steam generator, Boiler dynamics and control in nuclear power station. BNES, London (1979), 105-115.
[5] H.C. Unal, Density-wave oscillations in Sodium-heated once-through steam generator tubes, J. Heat Transfer 103 (1981).
[6] M. Kozeki et al., A study of helically-coiled tube once-through steam generator, Bulletin of the JSME 13(66) (1970) 1485-1494
[7] H. Nariai et al., Flow instabilities in a once-through steam generator, Boiler dynamics and control in nuclear power station. BNES, London (1979).
[8] H. Nariai et al., Friction pressure drop and heat transfer coefficient of two-phase flow in the helically coiled tube once-through steam generator for integrated type marine water reactor, J. Nuc. Sci. Tec. 19(11) (1982) 936~947.
[9] A. Clausse and R.T. Lahey, The analysis of periodic strange attractors during density-wave oscillations in boiling flows, Chaos, Solitions Fractals 1(2) (1991) 167-178
[10] C.J. Chang and R.T. Lahey, Analysis of chaotic instabilities in boiling systems, Nucl. Eng. Des. 167 (1997) 307-334.
[11] M. Furutera, Validity of homogeneous flow model for instability analysis, Nuc. Eng. Des. 96 (1986) 65-77
[12] F. Kreith, M. S. Bohn, Principles of heat transfer, Harper&Row publishers, New York, 1986
[13] Y. Mori and W. Nakayama, Study on forced convective heat transfer in curved pipes, Int. J. Mass Transfer 10 (1967) 37-59.
[14] M. Ishii, Study on flow instabilities in two-phase mixtures, ANL-76-23, 1976
[15] J. R. Rowland, Linear control systems, John Wiley & Sons, 1986

Table 1
Nariai's experimental condition

Geometric parameters	
Height of coiled tube (m)	1.3
Tube length (m)	61.2
Inner diameter of tube (m)	0.014
Outer diameter of tube (m)	0.02
Coiled diameter (m)	0.595
Number of tubes	4
Primary condition	
Pressure (Mpa)	11
Inlet temperature (^{o}C)	270~310
Mass flow rate (ton/h)	80
Secondary condition	
Outlet pressure (MPa)	2, 3, 5
Inlet sub-cooling (^{o}C)	44, 114, 194
Feedwater mass flow rate (kg/sec)	0.03~0.14
Inlet throttling coefficients	200 ~ 1500

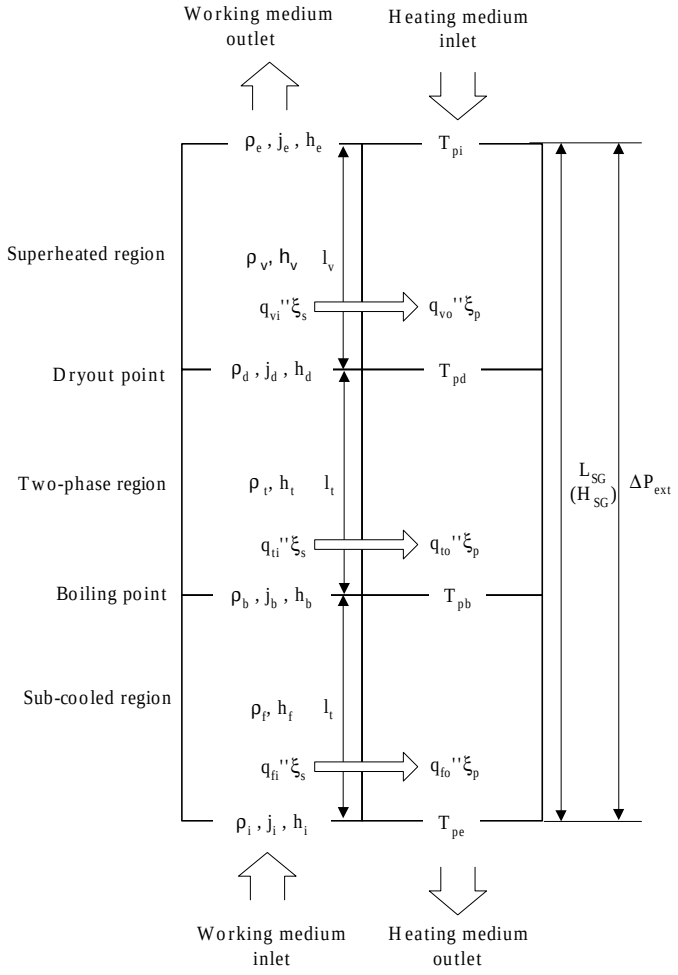

Fig. 1. Calculation domain and parameters used in this study

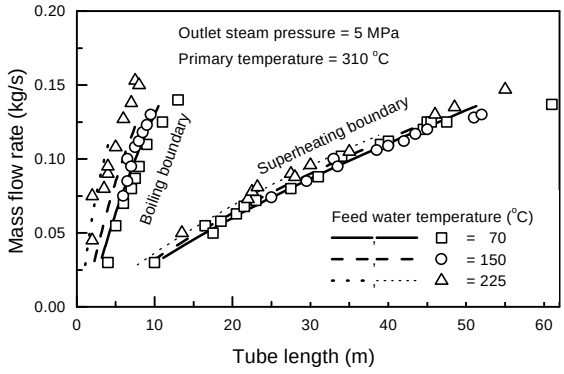

Fig. 2. The steady lengths of each regions as a function of feedwater mass flow rate

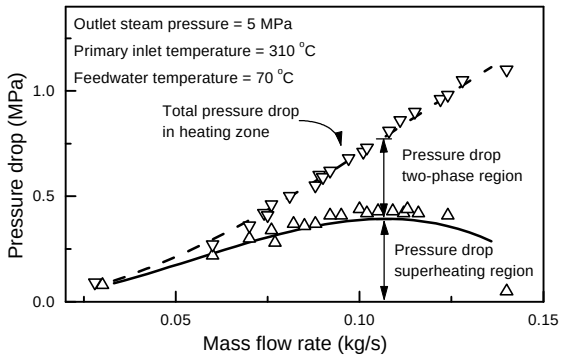

Fig 3. The steady pressure drops in the each regions as a function of feedwater mass flow rate

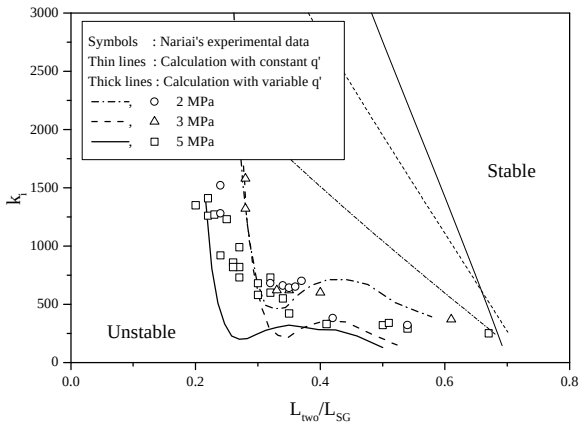

Fig. 4. Threshold inlet throttling coefficients as a function a L_{two}/L_{SG}